The 9th European Congress on Computational Methods in Applied Sciences and Engineering
ECCOMAS Congress 2024
3–7 June 2024, Lisboa, Portugal

PARAMETRIC MODEL REDUCTION FOR BROAD-BAND FREQUENCY ANALYSIS OF NEARLY PERIODIC STRUCTURES

J.-M. MENCIK

INSA Centre Val de Loire, Université d'Orléans, Université de Tours
Laboratoire de Mécanique Gabriel Lamé
Rue de la Chocolaterie, 41000 Blois, France
e-mail: jean-mathieu.mencik@insa-cvl.fr

Key words: Parametric model reduction, Substructures, Geometric changes, Matrix interpolation, Basis enrichment

Summary. This paper addresses the dynamic analysis of nearly periodic structures composed of substructures (cells) with varying properties. This may concern 2D or 3D substructures subjected to geometric modifications (mesh variations) or more standard parametric changes. In parametric model order reduction, reduced matrices of substructures can be interpolated over a multi-dimensional parametric space. Also, an interface reduction between the substructures can be proposed in which the vectors of interface degrees of freedom are described using the interface modes of an equivalent purely periodic structure. To improve the accuracy of the interpolation strategy at high frequencies, basis enrichment techniques are proposed. Within this framework, high-order static modes are used to enrich the basis of component modes of the substructures. Also, static correction vectors are used to enrich the basis of interface modes to account for the varying properties of the substructures.

1 INTRODUCTION

The dynamic behavior of nearly periodic structures with disordered substructures (cells) is investigated. This concerns 2D or 3D substructures subject to geometric changes (see Fig. 1) which can result from manufacturing process (variability) or design requirement, e.g., for the design of structures with low vibration levels. These geometric changes can represent any standard parametric variations (thicknesses) or mesh changes where shape functions and mesh parameters are introduced to move the nodes of a baseline finite element (FE) mesh. The mesh parameters are different between the substructures and, therefore, they can be randomly chosen to generate different substructures.

Reduced order models of substructures can be classically obtained using the Craig-Bampton (CB) method. Within this framework, reduced mass, damping and stiffness matrices of the substructures are obtained via Galerkin projection of the FE matrices onto the space of component modes (static and fixed interface modes). The issue with this method is the requirement that the component modes as well as the reduced matrices of the substructures be computed many times for different substructures, i.e., when parametric changes come into play. To solve this issue and quickly recompute the reduced substructure matrices, they can be interpolated over a parametric space. This means (i) expressing the reduced matrices at interpolation points (e.g.,

for some distorted FE meshes) in compatible coordinate systems [1], and (ii) interpolating the reduced matrices between the interpolation points, e.g., via standard Lagrangian interpolation functions. To improve the efficiency of the interpolation strategy, an interface reduction (between the substructures) for modeling a nearly periodic structure can be considered where the projection basis consists of the interface modes of the equivalent purely periodic structure.

Although efficient, the aforementioned interpolation strategy is prone to lack of accuracy at high frequencies. First, to express the reduced substructure matrices in compatible coordinate systems, only a few low-order fixed interface modes must be kept in the CB basis. Indeed high-order modes are usually associated with irregular shapes which make them difficult to correlate between two interpolation points. Next, the proposed interface reduction considers the interface modes of a purely periodic structure, which as such cannot account for geometric modifications. To improve the accuracy of the interpolation strategy, basis enrichment techniques are proposed in this paper. This consists in (i) enriching the CB basis of the substructures with high-order static modes and (ii) enriching the basis of interface modes with static correction vectors representing static response vectors that result from parametric changes.

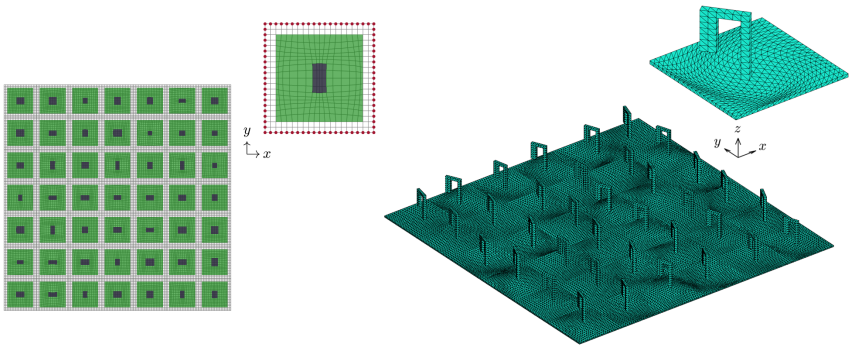

Figure 1: Examples of nearly periodic structures with 2D substructures (left) and 3D substructures (right).

2 MODEL REDUCTION BASED ON MATRIX INTERPOLATION

2.1 Reduced models of substructures

Examples of nearly periodic structures with 2D and 3D substructures with geometric changes are shown in Fig. 1. Those changes are here introduced by distorting the FE meshes of the substructures in the $(x,y)-$plane [2]. For a substructure s, this involves moving the positions of the nodes of a baseline/undistorted mesh (x_j^0, y_j^0) as follows:

$$x_j^s = x_j^0 + \sum_{k=1}^{n^x} \epsilon_{xk}^s f_{xk}(x_j^0, y_j^0) \quad , \quad y_j^s = y_j^0 + \sum_{k=1}^{n^y} \epsilon_{yk}^s f_{yk}(x_j^0, y_j^0), \tag{1}$$

where $f_{xk}(x,y)$ and $f_{yk}(x,y)$ are shape functions (similar between the substructures) which vanish at the boundary of the substructure, and ϵ_{xk}^s $(k=1,\ldots,n^x)$ and ϵ_{yk}^s $(k=1,\ldots,n^y)$ are mesh parameters (different between the substructures) which will be supposed to represent independent variables defined on supports $[-\delta_{xk}\,,\,\delta_{xk}]$ and $[-\delta_{yk}\,,\,\delta_{yk}]$ with dispersion parameters

δ_{xk} and δ_{yk}. Besides the substructure models may also depend on more standard parameters θ_k^s ($k = 1, \ldots, n^\theta$) (e.g., thickness, Young's modulus) defined as:

$$\theta_k^s = \theta_k^0 + \epsilon_{\theta k}^s \qquad k = 1, \ldots, n^\theta, \tag{2}$$

for some nominal values θ_k^0 and independent variables $\epsilon_{\theta k}^s$ defined on supports $[-\delta_{\theta k}\,,\,\delta_{\theta k}]$. Thus the dynamic equation of a substructure s subjected to parametric changes may be written in the frequency domain (frequency ω) as:

$$\left(-\omega^2 \mathbf{M}(\boldsymbol{\epsilon}^s) + \mathtt{i}\omega \mathbf{C}(\boldsymbol{\epsilon}^s) + \mathbf{K}(\boldsymbol{\epsilon}^s)\right) \mathbf{u}^s = \mathbf{F}^s, \tag{3}$$

with $\mathbf{u}^s$ and $\mathbf{F}^s$ the displacement and force vectors (respectively), and $\mathbf{M}(\boldsymbol{\epsilon}^s)$, $\mathbf{C}(\boldsymbol{\epsilon}^s)$ and $\mathbf{K}(\boldsymbol{\epsilon}^s)$ the mass, damping and stiffness matrices (respectively) where assumption is made that the damping matrix is of Rayleigh type, i.e., $\mathbf{C}(\boldsymbol{\epsilon}^s) = a\mathbf{M}(\boldsymbol{\epsilon}^s) + b\mathbf{K}(\boldsymbol{\epsilon}^s)$ for some constant damping parameters a and b. The vector of parameters is defined as $\boldsymbol{\epsilon}^s = [(\boldsymbol{\epsilon}_x^s)^T(\boldsymbol{\epsilon}_y^s)^T(\boldsymbol{\epsilon}_\theta^s)^T]^T$ with $\boldsymbol{\epsilon}_x^s = [\epsilon_{x1}^s \cdots \epsilon_{xn^x}^s]^T$ and $\boldsymbol{\epsilon}_y^s = [\epsilon_{y1}^s \cdots \epsilon_{yn^y}^s]^T$ the vectors of mesh parameters (distortion), and $\boldsymbol{\epsilon}_\theta^s = [\epsilon_{\theta 1}^s \cdots \epsilon_{\theta n^\theta}^s]^T$ the vector of parameters that concern other parametric changes.

Reduced models of the substructures can be expressed via the CB method, in which the displacement vector $\mathbf{u}^s$ is approximated as:

$$\mathbf{u}^s = \begin{bmatrix} \mathbf{u}_{\mathtt{B}}^s \\ \mathbf{u}_{\mathtt{I}}^s \end{bmatrix} \approx \begin{bmatrix} \mathbf{I} & \mathbf{0} \\ \mathbf{X}_{\mathtt{st}}(\boldsymbol{\epsilon}^s) & \widetilde{\mathbf{X}}(\boldsymbol{\epsilon}^s) \end{bmatrix} \begin{bmatrix} \widetilde{\mathbf{u}}_{\mathtt{B}}^s \\ \widetilde{\boldsymbol{\alpha}}^s \end{bmatrix} = \widetilde{\mathbf{T}}(\boldsymbol{\epsilon}^s)\widetilde{\mathbf{u}}^s, \tag{4}$$

where subscripts $\mathtt{B}$ and $\mathtt{I}$ refer to the boundary and internal degrees of freedom (DOFs), respectively. Here, $\widetilde{\mathbf{T}}(\boldsymbol{\epsilon}^s)$ is the CB transformation matrix, $\mathbf{X}_{\mathtt{st}}(\boldsymbol{\epsilon}^s)$ is the matrix of static modes defined by $\mathbf{X}_{\mathtt{st}}(\boldsymbol{\epsilon}^s) = -\mathbf{K}_{\mathtt{II}}(\boldsymbol{\epsilon}^s)^{-1}\mathbf{K}_{\mathtt{IB}}(\boldsymbol{\epsilon}^s)$, and $\widetilde{\mathbf{X}}(\boldsymbol{\epsilon}^s)$ is the reduced matrix of fixed interface modes — i.e., the eigenvectors of the matrix pencil $(\mathbf{K}_{\mathtt{II}}(\boldsymbol{\epsilon}^s), \mathbf{M}_{\mathtt{II}}(\boldsymbol{\epsilon}^s))$ — where only a small number $M_{\mathtt{I}}$ of these modes are retained, see [2]; also, $\widetilde{\boldsymbol{\alpha}}^s$ is the $M_{\mathtt{I}} \times 1$ vector of generalized coordinates for the fixed interface modes. The reduced substructure matrices are classically obtained through Galerkin projection onto the space of component modes, i.e., $\widetilde{\mathbf{M}}(\boldsymbol{\epsilon}^s) = \widetilde{\mathbf{T}}(\boldsymbol{\epsilon}^s)^T\mathbf{M}(\boldsymbol{\epsilon}^s)\widetilde{\mathbf{T}}(\boldsymbol{\epsilon}^s)$, $\widetilde{\mathbf{K}}(\boldsymbol{\epsilon}^s) = \widetilde{\mathbf{T}}(\boldsymbol{\epsilon}^s)^T\mathbf{K}(\boldsymbol{\epsilon}^s)\widetilde{\mathbf{T}}(\boldsymbol{\epsilon}^s)$ and $\widetilde{\mathbf{C}}(\boldsymbol{\epsilon}^s) = a\widetilde{\mathbf{M}}(\boldsymbol{\epsilon}^s) + b\widetilde{\mathbf{K}}(\boldsymbol{\epsilon}^s)$. Also, the reduced force vector is given by $\widetilde{\mathbf{F}}^s = \widetilde{\mathbf{T}}(\boldsymbol{\epsilon}^s)^T\mathbf{F}^s$ where $\widetilde{\mathbf{F}}^s$ is supposed to be parameter-independent (this can be verified if the internal DOFs of the substructures are free from excitation [3]).

To avoid computing the reduced matrices many times (for many different parameter vectors $\boldsymbol{\epsilon}^s$), they can be only expressed for a few parameter vectors $\boldsymbol{\epsilon}^s = \boldsymbol{\epsilon}_p$ with $p = 1, \ldots, n^p$ and n^p small. Then, the reduced substructure matrices for any parameter vector $\boldsymbol{\epsilon}^s$ can be approximated by matrix interpolation. At the "interpolation points" $\boldsymbol{\epsilon}_p$, the transformation matrix and the reduced matrices are expressed as:

$$\widetilde{\mathbf{T}}_p = \begin{bmatrix} \mathbf{I} & \mathbf{0} \\ (\mathbf{X}_{\mathtt{st}})_p & \widetilde{\mathbf{X}}_p \end{bmatrix} \quad , \quad \widetilde{\mathbf{M}}_p = \widetilde{\mathbf{T}}_p^T\mathbf{M}(\boldsymbol{\epsilon}_p)\widetilde{\mathbf{T}}_p \quad , \quad \widetilde{\mathbf{K}}_p = \widetilde{\mathbf{T}}_p^T\mathbf{K}(\boldsymbol{\epsilon}_p)\widetilde{\mathbf{T}}_p, \tag{5}$$

with $(\mathbf{X}_{\mathtt{st}})_p = \mathbf{X}_{\mathtt{st}}(\boldsymbol{\epsilon}_p)$ the matrices of static modes and $\widetilde{\mathbf{X}}_p = \widetilde{\mathbf{X}}(\boldsymbol{\epsilon}_p)$ the matrices of fixed interface modes which will be normalized so that $\widetilde{\mathbf{X}}_p^T\mathbf{M}_{\mathtt{II}}(\boldsymbol{\epsilon}_p)\widetilde{\mathbf{X}}_p = \mathbf{I}$. Prior to matrix interpolation, the reduced matrices $\widetilde{\mathbf{M}}_p$ and $\widetilde{\mathbf{K}}_p$ are to be expressed in compatible coordinate systems as

discussed in [1]. For this task, the following alternative matrices of fixed interface modes, at the interpolation points, can be considered:

$$\widehat{\mathbf{X}}_p = \widetilde{\mathbf{X}}_p(\boldsymbol{\Psi}^T\widetilde{\mathbf{X}}_p)^{-1}, \tag{6}$$

for some well-chosen matrix $\boldsymbol{\Psi}$. Here, the following simple expression of $\boldsymbol{\Psi}$ will be used:

$$\boldsymbol{\Psi} = \mathbf{M}^0_{\mathtt{II}}\widetilde{\mathbf{X}}^0. \tag{7}$$

To derive Eq. (7), a MAC-based correlation criterion can be invoked, see [3]. Thus the following alternative expressions for the transformation matrix and the reduced substructure matrices at the interpolation points are considered:

$$\widehat{\mathbf{T}}_p = \begin{bmatrix} \mathbf{I} & \mathbf{0} \\ (\mathbf{X}_{\mathtt{st}})_p & \widehat{\mathbf{X}}_p \end{bmatrix} \quad , \quad \widehat{\mathbf{M}}_p = \widehat{\mathbf{T}}_p^T\mathbf{M}(\boldsymbol{\epsilon}_p)\widehat{\mathbf{T}}_p \quad , \quad \widehat{\mathbf{K}}_p = \widehat{\mathbf{T}}_p^T\mathbf{K}(\boldsymbol{\epsilon}_p)\widehat{\mathbf{T}}_p. \tag{8}$$

The determination of the reduced mass and stiffness matrices of a substructure s, for a given parameter vector $\boldsymbol{\epsilon}^s$, follows from standard interpolation, i.e.,

$$\widehat{\mathbf{M}}(\boldsymbol{\epsilon}^s) = \widehat{\mathbf{M}}(\boldsymbol{\xi}^s) \approx \sum_{p=1}^{n^p} N_p(\boldsymbol{\xi}^s)\widehat{\mathbf{M}}_p \quad , \quad \widehat{\mathbf{K}}(\boldsymbol{\epsilon}^s) = \widehat{\mathbf{K}}(\boldsymbol{\xi}^s) \approx \sum_{p=1}^{n^p} N_p(\boldsymbol{\xi}^s)\widehat{\mathbf{K}}_p. \tag{9}$$

with $N_p(\boldsymbol{\xi}^s)$ Lagrangian interpolation functions and $\boldsymbol{\xi}^s$ parametric coordinates defined so that they are equal to one or zero at some points $\boldsymbol{\xi}_p$. These points coincide with the "physical" interpolation points $\boldsymbol{\epsilon}_p$ which will be defined as Gauss points.

2.2 Interface reduction

The dynamic equation of a whole nearly periodic structure composed of n^s substructures is obtained by assembling the reduced matrices $\widehat{\mathbf{M}}(\boldsymbol{\epsilon}^s)$, $\widehat{\mathbf{K}}(\boldsymbol{\epsilon}^s)$ and $\widehat{\mathbf{C}}(\boldsymbol{\epsilon}^s) = a\widehat{\mathbf{M}}(\boldsymbol{\epsilon}^s) + b\widehat{\mathbf{K}}(\boldsymbol{\epsilon}^s)$. This yields

$$\left(-\omega^2\widehat{\mathbf{M}}_{\mathtt{a}}(\boldsymbol{\epsilon}_{\mathtt{a}}) + \mathtt{i}\omega\widehat{\mathbf{C}}_{\mathtt{a}}(\boldsymbol{\epsilon}_{\mathtt{a}}) + \widehat{\mathbf{K}}_{\mathtt{a}}(\boldsymbol{\epsilon}_{\mathtt{a}})\right)\begin{bmatrix}(\widehat{\mathbf{u}}_{\mathtt{B}})_{\mathtt{a}} \\ \widehat{\boldsymbol{\alpha}}_{\mathtt{a}}\end{bmatrix} = \begin{bmatrix}(\mathbf{F}_{\mathtt{B}})_{\mathtt{a}} \\ \mathbf{0}\end{bmatrix}, \tag{10}$$

where $\boldsymbol{\epsilon}_{\mathtt{a}} = [(\boldsymbol{\epsilon}^1)^T \cdots (\boldsymbol{\epsilon}^{n^s})^T]^T$. Here, $(\widehat{\mathbf{u}}_{\mathtt{B}})_{\mathtt{a}}$ and $(\mathbf{F}_{\mathtt{B}})_{\mathtt{a}}$ denote the displacement and force vectors (respectively) at the interface between the substructures (the interface being defined as the union of the substructure boundaries). It should be noticed that, despite the CB-based reduced models of the substructures, the number of interface DOFs remains usually large. To address this issue, an interface reduction which uses the interface modes of the equivalent purely periodic structure (matrix $\widetilde{\mathbf{X}}^0_{\mathtt{a}}$) can be proposed. These modes represent the eigenvectors of the matrix pencil $((\widehat{\mathbf{K}}^0_{\mathtt{BB}})_{\mathtt{a}}, (\widehat{\mathbf{M}}^0_{\mathtt{BB}})_{\mathtt{a}})$ — where subscript 0 means that $\boldsymbol{\epsilon}_{\mathtt{a}} = \mathbf{0}$ (purely periodic case) — and can be classically normalized in such a way that $(\widetilde{\mathbf{X}}^0_{\mathtt{a}})^T(\widehat{\mathbf{M}}^0_{\mathtt{BB}})_{\mathtt{a}}\widetilde{\mathbf{X}}^0_{\mathtt{a}} = \mathbf{I}$ and $(\widetilde{\mathbf{X}}^0_{\mathtt{a}})^T(\widehat{\mathbf{K}}^0_{\mathtt{BB}})_{\mathtt{a}}\widetilde{\mathbf{X}}^0_{\mathtt{a}} = \widetilde{\boldsymbol{\Lambda}}^0_{\mathtt{a}}$ with $\widetilde{\boldsymbol{\Lambda}}^0_{\mathtt{a}}$ the diagonal matrix of the retained eigenvalues of $((\widehat{\mathbf{K}}^0_{\mathtt{BB}})_{\mathtt{a}}, (\widehat{\mathbf{M}}^0_{\mathtt{BB}})_{\mathtt{a}})$. To improve the accuracy of the interface reduction technique, it is proposed to enrich the basis of interface modes with residual flexibility vectors. Within this framework, the displacement vector $(\widehat{\mathbf{u}}_{\mathtt{B}})_{\mathtt{a}}$ is expressed as [3]:

$$(\widehat{\mathbf{u}}_{\mathtt{B}})_{\mathtt{a}} \approx \left[\widetilde{\mathbf{X}}^0_{\mathtt{a}} - \widetilde{\mathbf{G}}^0_{\mathtt{a}}(\widetilde{\boldsymbol{\Theta}}^0_{\mathtt{ex}})_{\mathtt{a}}(\mathbf{L}_{\mathtt{ex}})_{\mathtt{a}}\widetilde{\mathbf{X}}^0_{\mathtt{a}}\right]\widetilde{\boldsymbol{\beta}}_{\mathtt{a}} + \left[\widetilde{\mathbf{G}}^0_{\mathtt{a}}(\widetilde{\boldsymbol{\Theta}}^0_{\mathtt{ex}})_{\mathtt{a}}\right](\widehat{\mathbf{u}}_{\mathtt{ex}})_{\mathtt{a}}, \tag{11}$$

with $(\mathbf{L}_{\mathtt{ex}})_{\mathtt{a}}$ a Boolean matrix to localize the excitation DOFs and $\widetilde{\mathbf{G}}^0_{\mathtt{a}}$ the residual flexibility matrix defined by:

$$\widetilde{\mathbf{G}}^0_{\mathtt{a}} = \left((\widehat{\mathbf{K}}^0_{\mathtt{BB}})^{-1}_{\mathtt{a}} - \widetilde{\mathbf{X}}^0_{\mathtt{a}} (\widetilde{\boldsymbol{\Lambda}}^0_{\mathtt{a}})^{-1} (\widetilde{\mathbf{X}}^0_{\mathtt{a}})^T \right) (\mathbf{L}_{\mathtt{ex}})^T_{\mathtt{a}}. \tag{12}$$

Also, in Eq. (11), $(\widetilde{\boldsymbol{\Theta}}^0_{\mathtt{ex}})_{\mathtt{a}}$ is a square matrix of small size expressed by $(\widetilde{\boldsymbol{\Theta}}^0_{\mathtt{ex}})_{\mathtt{a}} = \left((\mathbf{L}_{\mathtt{ex}})_{\mathtt{a}} \widetilde{\mathbf{G}}^0_{\mathtt{a}} \right)^{-1}$. As a result, one obtains:

$$\begin{bmatrix} (\widehat{\mathbf{u}}_{\mathtt{B}})_{\mathtt{a}} \\ \widehat{\boldsymbol{\alpha}}_{\mathtt{a}} \end{bmatrix} \approx \begin{bmatrix} \widetilde{\mathbf{X}}^0_{\mathtt{a}} & \mathbf{0} \\ \mathbf{0} & \mathbf{I} \end{bmatrix} \begin{bmatrix} \widetilde{\boldsymbol{\beta}}_{\mathtt{a}} \\ \widehat{\boldsymbol{\alpha}}_{\mathtt{a}} \end{bmatrix} = \widetilde{\mathbf{T}}^0_{\mathtt{a}} \begin{bmatrix} \widetilde{\boldsymbol{\beta}}_{\mathtt{a}} \\ \widehat{\boldsymbol{\alpha}}_{\mathtt{a}} \end{bmatrix}, \tag{13}$$

with $\widetilde{\mathbf{X}}^0_{\mathtt{a}}$ the updated matrix of interface modes, and $\widetilde{\boldsymbol{\beta}}_{\mathtt{a}}$ the updated vector of generalized coordinates:

$$\widetilde{\mathbf{X}}^0_{\mathtt{a}} \leftarrow \left[\widetilde{\mathbf{X}}^0_{\mathtt{a}} - \widetilde{\mathbf{G}}^0_{\mathtt{a}} (\widetilde{\boldsymbol{\Theta}}^0_{\mathtt{ex}})_{\mathtt{a}} (\mathbf{L}_{\mathtt{ex}})_{\mathtt{a}} \widetilde{\mathbf{X}}^0_{\mathtt{a}} \quad \widetilde{\mathbf{G}}^0_{\mathtt{a}} (\widetilde{\boldsymbol{\Theta}}^0_{\mathtt{ex}})_{\mathtt{a}} \right] \quad \text{and} \quad \widetilde{\boldsymbol{\beta}}_{\mathtt{a}} \leftarrow \begin{bmatrix} \widetilde{\boldsymbol{\beta}}_{\mathtt{a}} \\ (\widehat{\mathbf{u}}_{\mathtt{ex}})_{\mathtt{a}} \end{bmatrix}. \tag{14}$$

The reduced dynamic equation of the nearly periodic structure is obtained by projecting the matrices $\widehat{\mathbf{M}}_{\mathtt{a}}(\boldsymbol{\epsilon}_{\mathtt{a}})$, $\widehat{\mathbf{C}}_{\mathtt{a}}(\boldsymbol{\epsilon}_{\mathtt{a}})$ and $\widehat{\mathbf{K}}_{\mathtt{a}}(\boldsymbol{\epsilon}_{\mathtt{a}})$ onto the column space of $\widetilde{\mathbf{T}}^0_{\mathtt{a}}$.

3 MODEL REDUCTION WITH BASIS ENRICHMENT

Although efficient (computational saving), the model reduction strategy proposed in Sec. 2 suffers from numerical limitations and lack of accuracy, especially at high frequencies, for the following reasons:

- To interpolate the reduced substructure matrices between interpolation points (see Sec. 2.1), the column spaces of the matrices $\widetilde{\mathbf{X}}_p$ have to be "sufficiently close" to the column space of the matrix $\boldsymbol{\Psi}$ as expressed by Eq. (7). This particularly means only considering a few low-order fixed interface modes in the reduced matrices $\widetilde{\mathbf{X}}_p$.
- In the interface reduction method proposed in Sec. 2.2, the reduced matrix of interface modes $\widetilde{\mathbf{X}}^0_{\mathtt{a}}$ of an equivalent purely periodic structure is used. In this sense, these interface modes do not account for the parametric changes of the substructures and, therefore, the convergence of this mode basis cannot be guaranteed.

To solve these issues, two basis enrichment techniques are proposed (see hereafter).

3.1 High-order static modes

To improve the accuracy of the interpolation strategy at high frequencies, high-order static correction terms can be considered to enrich the CB basis of the substructures. Indeed the quasi-static response of the substructures associated with the residual fixed interface modes which are not retained in the CB basis can be approximated as $(\mathbf{u}^s_{\mathtt{I}})_{\mathtt{r}} \approx \omega^2 \mathbf{X}^{\mathtt{cor}}_{\mathtt{st}} \mathbf{u}^s_{\mathtt{B}}$ with $\mathbf{X}^{\mathtt{cor}}_{\mathtt{st}}$ a matrix of high-order static modes given by [4]:

$$\mathbf{X}^{\mathtt{cor}}_{\mathtt{st}} = \left(\mathbf{K}^{-1}_{\mathtt{II}} - \widetilde{\mathbf{X}} \widetilde{\boldsymbol{\Lambda}}^{-1} \widetilde{\mathbf{X}}^T \right) (\mathbf{M}_{\mathtt{II}} \mathbf{X}_{\mathtt{st}} + \mathbf{M}_{\mathtt{IB}}), \tag{15}$$

where the dependency on parameters $\boldsymbol{\epsilon}^s$ has been dropped for the sake of conciseness. Here, $\widetilde{\mathbf{X}}$ and $\widetilde{\boldsymbol{\Lambda}}$ denote, respectively, the reduced matrix of fixed interface modes of a substructure and

the related reduced diagonal matrix of eigenvalues. The fact that $(\mathbf{u}_{\mathtt{I}}^s)_{\mathtt{r}} \approx \omega^2 \mathbf{X}_{\mathtt{st}}^{\mathtt{cor}} \mathbf{u}_{\mathtt{B}}^s$ means that $(\mathbf{u}_{\mathtt{I}}^s)_{\mathtt{r}}$ is located in the column space of $\mathbf{X}_{\mathtt{st}}^{\mathtt{cor}}$, and then that the column vectors of $\mathbf{X}_{\mathtt{st}}^{\mathtt{cor}}$ can be used to enrich the CB basis. For computational purposes, it is advised to consider orthogonal vectors from a reduced singular value decomposition (SVD) of $\mathbf{X}_{\mathtt{st}}^{\mathtt{cor}}$:

$$\mathbf{X}_{\mathtt{st}}^{\mathtt{cor}} \approx \widetilde{\mathbf{U}} \widetilde{\mathbf{\Sigma}} \widetilde{\mathbf{V}}^T, \tag{16}$$

with $\widetilde{\mathbf{\Sigma}}$ a reduced matrix consisting of the $M_{\mathtt{st}}^{\mathtt{e}}$ highest singular values of $\mathbf{X}_{\mathtt{st}}^{\mathtt{cor}}$, and $\widetilde{\mathbf{U}}$ and $\widetilde{\mathbf{V}}$ the related orthogonal matrices of singular vectors. From Eq. (16), it appears that the column vectors of $\widetilde{\mathbf{U}}$ constitute a relevant basis for the column space of $\mathbf{X}_{\mathtt{st}}^{\mathtt{cor}}$. Following the interpolation strategy proposed in Sec. 2.1, reduced matrices of left singular vectors $\widetilde{\mathbf{U}}_p$ are considered at interpolation points "$\boldsymbol{\epsilon}_p$". These matrices need to be expressed in compatible coordinate systems in the same way as in Eq. (6), i.e.,

$$\widehat{\mathbf{U}}_p = \widetilde{\mathbf{U}}_p \left((\widetilde{\mathbf{U}}^0)^T \widetilde{\mathbf{U}}_p \right)^{-1}, \tag{17}$$

where $\widetilde{\mathbf{U}}_p$ and $\widetilde{\mathbf{U}}^0$ represent $\widetilde{\mathbf{U}}$ when $\boldsymbol{\epsilon}^s = \boldsymbol{\epsilon}_p$ and $\boldsymbol{\epsilon}^s = \mathbf{0}$, respectively. As a result, the transformation matrices and the reduced substructure matrices at the interpolation points become, see Eq. (8):

$$\widehat{\mathbf{T}}_p = \begin{bmatrix} \mathbf{I} & \mathbf{0} & \mathbf{0} \\ (\mathbf{X}_{\mathtt{st}})_p & \widehat{\mathbf{X}}_p & \widehat{\mathbf{U}}_p \end{bmatrix} \quad , \quad \widehat{\mathbf{M}}_p = \widehat{\mathbf{T}}_p^T \mathbf{M}(\boldsymbol{\epsilon}_p) \widehat{\mathbf{T}}_p \quad , \quad \widehat{\mathbf{K}}_p = \widehat{\mathbf{T}}_p^T \mathbf{K}(\boldsymbol{\epsilon}_p) \widehat{\mathbf{T}}_p. \tag{18}$$

3.2 Static correction of interface modes

Let us consider the following matrix of residual force vectors resulting from parametric changes [5]:

$$\Delta(\mathbf{F}_{\mathtt{B}})_{\mathtt{a}} = -\Delta(\widehat{\mathbf{K}}_{\mathtt{BB}})_{\mathtt{a}} \, \widetilde{\mathbf{X}}_{\mathtt{a}}^0. \tag{19}$$

Here, $\Delta(\widehat{\mathbf{K}}_{\mathtt{BB}})_{\mathtt{a}}$ denotes the perturbation of the stiffness matrix (interface DOFs) due to parametric changes:

$$\Delta(\widehat{\mathbf{K}}_{\mathtt{BB}})_{\mathtt{a}} = (\widehat{\mathbf{K}}_{\mathtt{BB}})_{\mathtt{a}}(\boldsymbol{\epsilon}_{\mathtt{a}}) - (\widehat{\mathbf{K}}_{\mathtt{BB}}^0)_{\mathtt{a}}, \tag{20}$$

with $(\widehat{\mathbf{K}}_{\mathtt{BB}})_{\mathtt{a}}(\boldsymbol{\epsilon}_{\mathtt{a}})$ and $(\widehat{\mathbf{K}}_{\mathtt{BB}}^0)_{\mathtt{a}}$ the stiffness matrices for the interface DOFs of the nearly periodic structure ($\boldsymbol{\epsilon}_{\mathtt{a}} \neq \mathbf{0}$) and the purely periodic one ($\boldsymbol{\epsilon}_{\mathtt{a}} = \mathbf{0}$), respectively. From Eq. (19), the following matrix of static correction vectors due to parametric changes can be proposed to enrich the basis of interface modes:

$$\Delta\widetilde{\mathbf{X}}_{\mathtt{a}} = (\widehat{\mathbf{K}}_{\mathtt{BB}}^0)_{\mathtt{a}}^{-1} \, \Delta(\mathbf{F}_{\mathtt{B}})_{\mathtt{a}} = -(\widehat{\mathbf{K}}_{\mathtt{BB}}^0)_{\mathtt{a}}^{-1} \, \Delta(\widehat{\mathbf{K}}_{\mathtt{BB}})_{\mathtt{a}} \, \widetilde{\mathbf{X}}_{\mathtt{a}}^0. \tag{21}$$

A SVD of the matrix $\Delta\widetilde{\mathbf{X}}_{\mathtt{a}}$ can be performed as:

$$\Delta\widetilde{\mathbf{X}}_{\mathtt{a}} = \mathbf{U}_{\mathtt{a}} \mathbf{\Sigma}_{\mathtt{a}} \mathbf{V}_{\mathtt{a}}^T. \tag{22}$$

Here, $\mathbf{U}_{\mathtt{a}}$ is an orthogonal matrix of left singular vectors that span the same vector space as $\Delta\widetilde{\mathbf{X}}_{\mathtt{a}}$ and which can therefore be used as alternative static correction vectors. Hence, the following updated matrix of interface modes can be considered to improve the accuracy of the proposed approach:

$$\widetilde{\mathbf{X}}_{\mathtt{a}}^0 \leftarrow \left[\widetilde{\mathbf{X}}_{\mathtt{a}}^0 \quad \mathbf{U}_{\mathtt{a}} \right]. \tag{23}$$

Note that the matrix $\mathbf{U}_{\mathtt{a}}$ contains the same number of vectors as $\widetilde{\mathbf{X}}_{\mathtt{a}}^0$, i.e., the updated matrix of interface modes contains twice the number of vectors of the original matrix.

4 NUMERICAL RESULTS

4.1 Nearly periodic structure with 3D substructures

In this example, a nearly periodic structure with 4×4 3D substructures, clamped at its four edges, is considered as shown in Fig. 2. Each substructure consists of a square-base (surface area 0.07×0.07 m^2) supporting a hanger arm which behaves as a multi-DOF resonator. The related material properties are: density $\rho = 2700$ kg.m^{-3}, Young's modulus $E = 70$ GPa and Poisson's ratio $\nu = 0.3$. The FE meshes and FE models of the baseline substructure and the distorted substructures are generated with COMSOL and MATLAB using in-house codes. The substructure mesh is built from 10-node quadratic tetrahedrons that involves $16,533$ internal DOFs and 1512 boundary DOFs. Mesh variations involve changing the angle of the hanger arm as well as moving its position in the (x,y) plane. For that purpose, three mesh parameters — i.e., ϵ_1^s (for the angle), ϵ_{x2}^s and ϵ_{y2}^s (for the positions along the $x-$ and $y-$ directions) — are considered. In this case the nodes of the baseline substructure are moved as follows:

$$x_j^s = x_j^0 + \epsilon_1^s f_{x1}(x_j^0, y_j^0) + \epsilon_{x2}^s f_{x2}(x_j^0, y_j^0) \quad , \quad y_j^s = y_j^0 + \epsilon_1^s f_{y1}(x_j^0, y_j^0) + \epsilon_{y2}^s f_{y2}(x_j^0, y_j^0), \tag{24}$$

with $f_{x1}(x,y)$, $f_{y1}(x,y)$, $f_{x2}(x,y)$ and $f_{y2}(x,y)$ four shape functions. Here, a 3D interpolation scheme based on $3 \times 3 \times 3$ interpolation points and 27 quadratic Lagrange polynomials $N_p(\xi^s, \eta^s, \zeta^s)$ $(p = 1, \ldots, 27)$ is considered. For the sake of clarity, a schematic of the distorted meshes of the substructures at some interpolation points (9 points among 27) is given in Fig. 3.

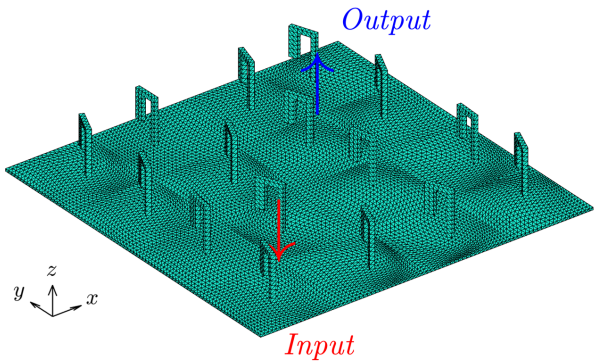

Figure 2: Nearly periodic structure with 3D substructures (each substructure consists of a square-base supporting a hanger arm with varying angle and positions).

The nearly periodic structure is excited by a unit harmonic force acting downward (input) at some substructure corner as shown in Fig. 2. The resulting quadratic velocity (output) — i.e., $\omega^2 |w_{\mathtt{out}}|^2$ with $w_{\mathtt{out}}$ the $z-$displacement — at another corner (see Fig. 2) is assessed. First, the FE-based reference frequency responses of the nearly and purely periodic structures are computed over $[0\,,\,2500]$ Hz as shown in Fig. 4. In this frequency range, the baseline substructure reveals four eigenfrequencies $f_1 = 722$ Hz, $f_2 = 760$ Hz, $f_3 = 1468$ Hz and $f_4 = 1573$ Hz. Concerning the purely periodic structure, low vibration levels occur in the vicinity of the resonance frequencies f_1 and f_2 which are associated with band gap phenomena. Regarding the nearly periodic structure, the response function shows irregular behavior especially after 1000 Hz where many local resonance peaks occur.

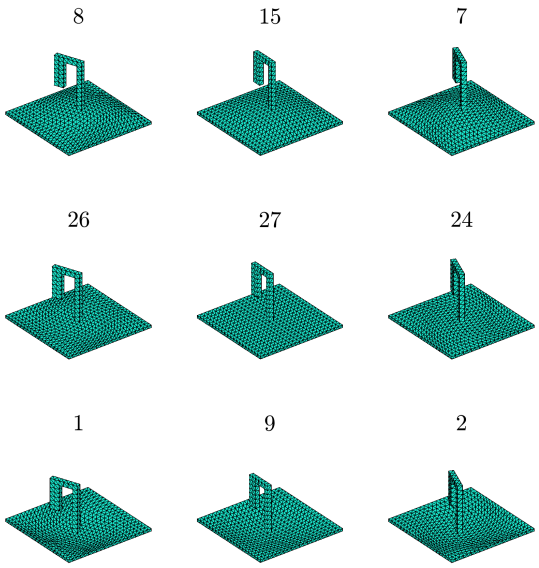

Figure 3: FE meshes of the substructures at some interpolation points (first example).

With the classic interpolation strategy (see Sec. 2), the harmonic behavior of the nearly periodic structure can be predicted. Within this framework, a CB approximation for the internal DOFs of the substructures with $M_{\mathtt{I}} = 6$ fixed interface modes is considered. The procedure to select these modes consists in retaining those whose eigenfrequencies are less than twice the maximum frequency of interest, i.e., below 5000 Hz. Also, a reduction of the number of interface DOFs, between the substructures, is proposed as explained in Sec. 2.2. In this case, $100 + 1$ modes — representing the standard interface modes and one additional residual term corresponding to the excitation DOF, see Eq. (14) — are considered. Fig. 5 shows a comparison between the proposed solution and the reference one. An insight into the high frequency range [1500 , 2500] Hz is also proposed (see bottom figure) where it becomes clear that the interpolation strategy suffers from a lack of accuracy in this range.

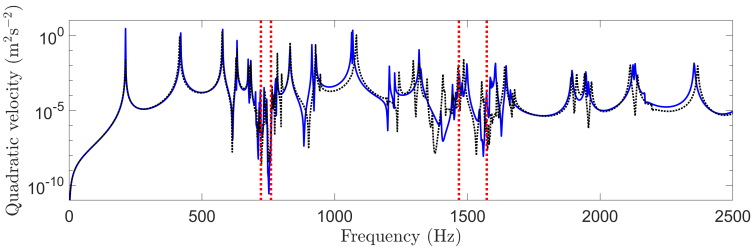

Figure 4: Frequency responses (first example): reference solutions for the purely periodic structure (blue solid line) and the nearly periodic structure (black dotted line). Red dotted vertical lines indicate the eigenfrequencies of the baseline substructure with clamped boundary.

To address the lack of accuracy of the interpolation strategy, the basis enrichment techniques proposed in Secs. 3.1 and 3.2 are considered. Within this framework, the CB basis of the substructures at the interpolation points is enriched with $M^{\mathtt{e}}_{\mathtt{st}} = 12$ high-order static modes. In

addition, the interface modes of the structure are enriched with static correction vectors, see Eq. (23). Note that, by definition, the number of these static correction vectors corresponds to the number of interface modes, i.e., 101. By considering the interpolation strategy with basis enrichment, the frequency response can be accurately predicted over the whole frequency range as shown in Fig. 6, even at high frequencies (as expected). Slight errors can be observed close to the band gap regions, which are however associated with low vibration levels. For the sake of clarity, the sizes of the full and reduced models are detailed in Tab. 1. In terms of computational time, the interpolation strategies yield a drastic reduction, i.e., around 99.9% time saving to compute the frequency response.

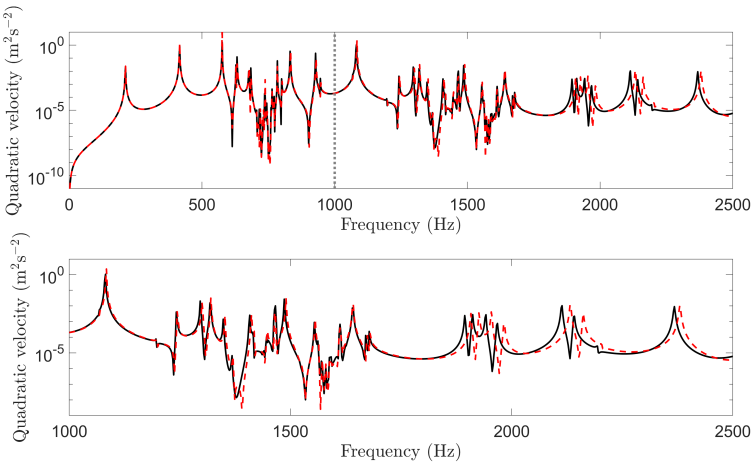

Figure 5: Frequency responses of the nearly periodic structure (first example): reference solution (black solid line) and proposed solution without basis enrichment (red dashed line) over [0 , 2500] Hz (top) and [1000 , 2500] Hz (bottom).

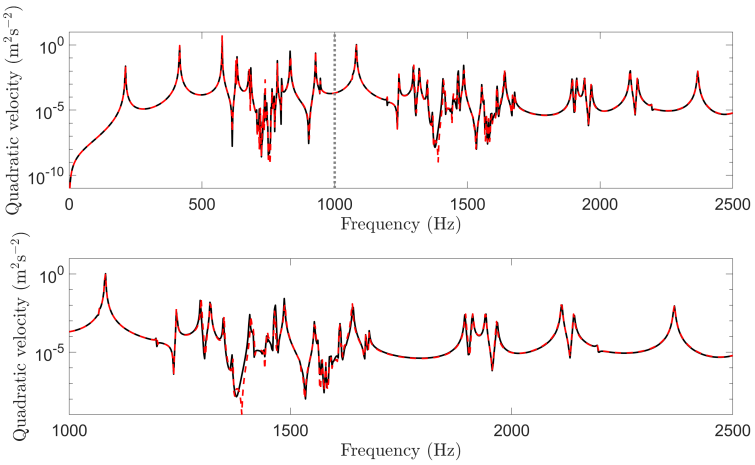

Figure 6: Frequency responses of the nearly periodic structure (first example): reference solution (black solid line) and proposed solution with basis enrichment (red dashed line) over [0 , 2500] Hz (top) and [1000 , 2500] Hz (bottom).

Table 1: Number of DOFs involved in the models (first example).

	Reference	Interpolated	Interpolated with basis enrichment
Substructure	Boundary: 1512 Internal: $16,533$	Static modes: 1512 Fixed interface modes: 6	Static modes: 1512 Fixed interface modes: 6 High-order static modes: 12
Interface	8937	Interface modes: 101	Interface modes: 101 Static correction vectors: 101
Structure	$273,465$	$101 + 16 \times 6 = 197$	$202 + 16 \times (6 + 12) = 490$

4.2 Industrial bladed disk

This example discusses the dynamic behavior of an industrial bladed disk with $n^s = 24$ sectors (see Fig. 7) representing 3D substructures subjected to an engine order excitation. Within this framework, the tips of the blades are subjected to harmonic forces of magnitudes $e^{-\mathtt{i}(s-1)\frac{2\pi \mathrm{EO}}{n^s}}$ ($s = 1, \ldots, n^s$) — EO being the engine order of the excitation — in the circumferential direction. The main characteristics of the structure are: inner and outer radii of the disk of 50 mm and 212 mm (respectively), radius of the tips of the blades of 280 mm, density $\rho = 7800$ kg.m^{-3}, Young's modulus $E = 200$ GPa and Poisson's ratio $\nu = 0.25$. The FE mesh of the whole structure is built from 20-node quadratic hexahedrons and $192,096$ DOFs. Also, the FE mesh of a substructure (see Fig. 7) involves 8730 DOFs including $n = 2 \times 726$ DOFs on the coupling interfaces with the connected substructures. In this example, the boundary DOFs of a substructure represent those on the coupling interfaces and the excitation DOF (tip of the blade). As a result, the interface DOFs of the bladed disk represent the DOFs on the coupling interfaces between the substructures, and the excitation DOFs ($n^s = 24$ DOFs). A common industrial situation concerns the analysis of mistuned bladed disks where the Young's modulus of each blade is perturbed [6], i.e., $E^s_{\mathtt{bl}} = E^0_{\mathtt{bl}} + \epsilon^s$ where, in the present case, ϵ^s ($s = 1, \ldots, n^s$) represent independent random variables with support $\pm 0.025 E^0_{\mathtt{bl}}$. In this case, a simple 1D interpolation scheme based on 3 points and 3 quadratic Lagrange polynomials $N_p(\xi^s)$ ($p = 1, \ldots, 3$) is enough to approximate the reduced substructure matrices.

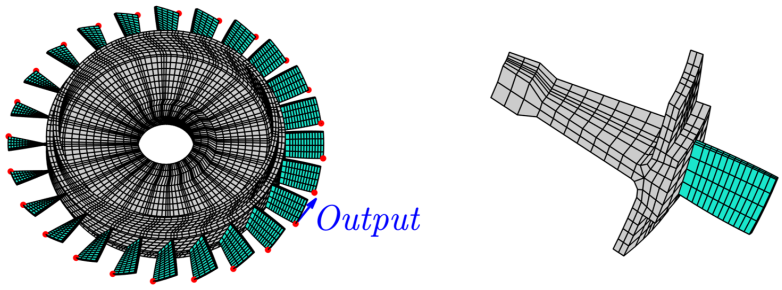

Figure 7: Bladed disk with 3D substructures (left) and related substructure (right). Red dots denote excitation DOFs; Green parts denote blades.

The quadratic velocity about the circumferential direction at the tip of the substructure 1 (see Fig. 7) is assessed when EO = 3. The FE-based reference frequency responses of the purely periodic (tuned) and nearly periodic (mistuned) structures are computed over [0 , 5000] Hz as shown in Fig. 8 where the mistuning effect can be well observed. Indeed, the resonance peaks

for the tuned and mistuned structures appear to be strongly dissimilar after 1500 Hz.

With the classic interpolation strategy, the harmonic behavior of the mistuned bladed disk can be predicted as shown in Fig. 9. Here, a CB approximation for the internal DOFs of the substructures with $M_{\mathtt{I}} = 7$ fixed interface modes is considered. Also, a reduction of the number of interface DOFs is performed (see Sec. 2.2) where 100+24 interface modes are considered. Again, it appears that the interpolation strategy suffers from a lack of accuracy, e.g., for capturing the resonance peaks at high frequencies as well as other resonance peaks at low frequencies (between 1500 Hz and 2500 Hz) that result from mistuning.

To address the lack of accuracy of the interpolation strategy, the basis enrichment techniques proposed in Secs. 3.1 and 3.2 are considered. In this case, $M^{\mathtt{e}}_{\mathtt{st}} = M_{\mathtt{I}} = 7$ high-order static modes (CB basis) and 124 static correction vectors (basis of interface modes) are used (see Tab. 2 for the sizes of the full FE model and the reduced models). The predicted response function is plotted in Fig. 10. Again, the proposed solution correctly matches the reference one over the whole frequency band. This further demonstrates the potential of the proposed approach to handle complex problems of engineering concern.

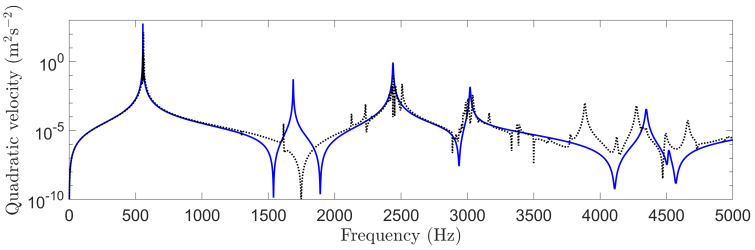

Figure 8: Frequency responses (second example): reference solutions for the purely periodic structure (blue solid line) and the nearly periodic structure (black dotted line).

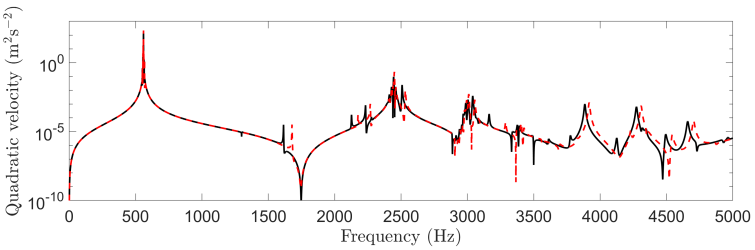

Figure 9: Frequency responses of the nearly periodic structure (second example): reference solution (black solid line) and proposed solution without basis enrichment (red dashed line).

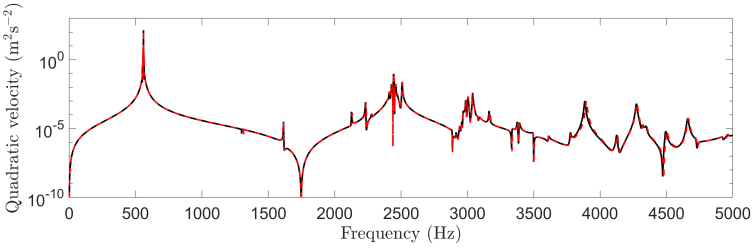

Figure 10: Frequency responses of the nearly periodic structure (second example): reference solution (black solid line) and proposed solution with basis enrichment (red dashed line).

Table 2: Number of DOFs involved in the models (second example).

	Reference	Interpolated	Interpolated with basis enrichment
Substructure	Boundary: 1453 Internal: 7277	Static modes: 1453 Fixed interface modes: 7	Static modes: 1453 Fixed interface modes: 7 High-order static modes: 7
Interface	$17,448$	Interface modes: 124	Interface modes: 124 Static correction vectors: 124
Structure	$192,096$	$124 + 24 \times 7 = 292$	$248 + 24 \times (7 + 7) = 584$

5 CONCLUSION

A reduced order model strategy has been proposed for the dynamic analysis of nearly periodic structures with parameter-dependent substructure models. Within this framework, reduced substructure matrices are interpolated over a parametric space. Next, an interface reduction, between the substructures, based on the interface modes of an equivalent purely periodic structure has been considered. To improve the accuracy of the strategy, basis enrichment techniques have been proposed that consist in (i) using high-order static modes to enrich the basis of component modes (CB) of the substructures and (ii) using static correction vectors which account for parametric changes to enrich the basis of interface modes. Numerical experiments have been carried out which have clearly highlighted the relevance of the proposed approach.

ACKNOWLEDGMENTS

The author thanks Safran for providing the FE model of the bladed disk presented in Sec. 4.2.

REFERENCES

[1] H. Panzer, J. Mohring, R. Eid, B. Lohmann, Parametric model order reduction by matrix interpolation, at-Automatisierungstechnik 58 (8) (2010) 475–484. doi:10.1524/auto.2010.0863.

[2] J.-M. Mencik, Model reduction based on matrix interpolation and distorted finite element meshes for dynamic analysis of 2D nearly periodic structures, Finite Elements in Analysis and Design 188 (2021) 103518. doi:10.1016/j.finel.2021.103518.

[3] J.-M. Mencik, Improved model reduction with basis enrichment for dynamic analysis of nearly periodic structures including substructures with geometric changes, Journal of Computational and Applied Mathematics 445 (2024) 115844. doi:10.1016/j.cam.2024.115844.

[4] D. Rixen, High order static correction modes for component mode synthesis, Proceedings of the Fifth World Congress on Computational Mechanics (WCCM), Vienna, Austria (2002).

[5] J.-M. Mencik, N. Bouhaddi, Dynamic reanalysis of structures with geometric variability and parametric uncertainties via an adaptive model reduction method, Mechanical Systems and Signal Processing 190 (2021) 110127. doi:10.1016/j.ymssp.2023.110127.

[6] M. Castanier, G. Ottarsson, C. Pierre, A reduced order modeling technique for mistuned bladed disks, Journal of Vibration and Acoustics 119 (3) (1997) 439–447. doi:10.1115/1.2889743.